Optical Superradiance from Nuclear Spin Environment of Single-Photon Emitters

E. M. Kessler,[1] S. Yelin,[2,3] M. D. Lukin,[3,4] J. I. Cirac,[1] and G. Giedke[1]

[1]*Max-Planck-Institut für Quantenoptik, Hans-Kopfermann-Strasse 1, D-85748 Garching, Germany*
[2]*Department of Physics, University of Connecticut, Storrs, Connecticut 06269, USA*
[3]*ITAMP, Harvard-Smithsonian Center for Astrophysics, Cambridge, Massachusetts 02138, USA*
[4]*Department of Physics, Harvard University, Cambridge, Massachusetts 02138, USA*

(Received 8 February 2010; published 9 April 2010)

We show that superradiant optical emission can be observed from the polarized nuclear spin ensemble surrounding a single-photon emitter such as a single quantum dot or nitrogen-vacancy center. The superradiant light is emitted under optical pumping conditions and would be observable with realistic experimental parameters.

DOI: 10.1103/PhysRevLett.104.143601 PACS numbers: 42.50.Nn, 78.67.−n

Superradiance (SR) is a cooperative radiation effect resulting from spontaneous buildup and reinforcement of correlations between initially independent dipoles. Its most prominent feature is an emission intensity burst in which the system radiates much faster than an otherwise identical system of independent emitters. This phenomenon is of fundamental importance in quantum optics and since its first prediction by Dicke in 1954 [1] it has been studied extensively (for a review see [2]). The rich steady state properties of the associated dynamics can account for strong correlation effects including phase transitions and bistability [3,4]. Yet in its original form optical SR is difficult to observe due to dephasing dipole-dipole van der Waals interactions, which suppress a coherence buildup in atomic ensembles.

In this Letter, we show that cooperative emission can occur from the ensemble of nuclear spins surrounding a quantum emitter such as a self-assembled quantum dot (QD) or an nitrogen- vacancy (NV) center. The interaction of the nuclear spin ensemble and optical field is mediated by the electron spin of the emitter. Because of the indirect character of the interaction, the dephasing van der Waals interactions vanish in this setting.

We first explain the proposal using the example of an NV center in a diamond. Then, we adapt the model to QDs, which promise strong effects due to the large number of involved nuclei. Despite the inhomogeneity of the nuclear spin coupling and related dephasing processes, we predict a SR-like correlation buildup in the nuclear spin ensemble and a significant intensity burst of several orders of magnitude in the optical emission profile. Finally, we point out the possibility of observing phase transitions and bistability in the nuclear system.

The superradiant effect is based on the collective hyperfine (HF) interaction of the electronic spin of the defect (QD or NV) with N initially polarized proximal nuclear spins. It is dominated by the isotropic contact term [5,6] and reads in an external magnetic field ($\hbar = 1$):

$$H = \frac{g}{2}(A^+S^- + A^-S^+) + gA^zS^z + \omega_S S^z. \qquad (1)$$

Here S^μ and $A^\mu = \sum_{i=1}^N g_i \sigma_i^\mu$ ($\mu = +, -, z$) denote electron and collective nuclear spin operators, respectively. The coupling coefficients are normalized such that $\sum_i g_i^2 = 1$ and individual nuclear spin operators σ_i^μ are assumed to be spin $1/2$ for simplicity; g gives the overall HF coupling strength and ω_S denotes the electron Zeeman splitting. We neglect the typically very small nuclear Zeeman and nuclear dipole-dipole terms.

Let us first consider NV centers, in which the effect can be studied in a clean and relatively small spin environment. Because of their extraordinary quantum properties, such as ultralong decoherence times even at room temperature, NV centers have attracted wide interest [7] resulting, e.g., in the demonstration of entanglement and quantum gates between the electron and proximal nuclear spins [8]. Both the NV center's electronic ground (^3A) and optically excited states (^3E) are spin triplet ($S = 1$) [7]. In the absence of a magnetic field, the ground state sublevels $|m_S = \pm 1\rangle$ are split from $|m_S = 0\rangle$. In the following, we assume that a B field is applied along the NV axis to bring $|m_S = 0\rangle$ and $|m_S = 1\rangle$ close to degeneracy [9]. In this case, $|m_S = -1\rangle$ is off resonance and can be disregarded. We focus on low-strain NV centers with well-defined selection rules and assume that it is optically excited by selectively driving the weakly allowed transition from $|m_S = 1\rangle$ to a state $|E_x\rangle$ in the ^3E manifold which decays primarily into $|m_S = 0\rangle$ [10]; see Fig. 1(a). The nuclear spin environment of the NV center consists of proximal ^{13}C ($I = 1/2$) nuclei in the otherwise spinless ^{12}C matrix, which are HF coupled to the electronic spin of the defect center. The interaction is dominated by the Fermi-contact term such that the coupling is isotropic (to first order) and described by Eq. (1) (ω_S here contains both zero-field splitting and Zeeman energy). Nevertheless in the simulations conducted below, we included the small anisotropic dipole-dipole terms.

We describe now the coupling of the nuclear spin to the optical field as depicted in Fig. 1(b). It is best understood as a two-step process: first, strongly driving a dipole-forbidden optical transition of the $|m_S = 1\rangle$ spin state

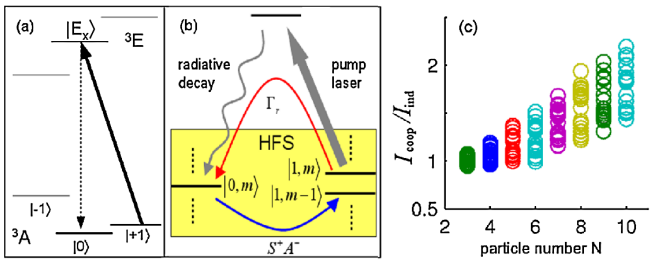

FIG. 1 (color online). (a) Simplified level scheme of NV center with relevant Λ system (cf. the text and [10]). (b) Sketch of relevant processes: electronic ground states are coupled by optical pumping and HF flipflops; the states are labeled by the z components of the electron and nuclear spin. (c) $I_{\mathrm{coop}}/I_{\mathrm{ind}}$ for randomly chosen nuclear environments of an NV center. The first nuclear shell is taken to be spinless, as due to their very strong coupling they would evolve largely independent from the ensemble.

(the allowed transition is far off resonant) pumps the electron into $|m_S = 0\rangle$. Such Raman spin-flip transitions have been demonstrated recently [10]. Since the short-lived excited state is populated negligibly throughout the process, we can eliminate it from the dynamics using standard techniques and obtain a master equation for the electron spin decaying with effective rate Γ_r:

$$\dot{\rho} = \Gamma_r(S^-\rho S^+ - \tfrac{1}{2}S^+S^-\rho - \tfrac{1}{2}\rho S^+S^-) - i[H, \rho], \quad (2)$$

each decay being accompanied by a Raman photon. Second, the return to state $|m_S = 1\rangle$, necessary for the next emission, occurs through H via a HF mediated electron spin flip (and nuclear spin flop). Thus, each Raman photon indicates a nuclear spin flop and the emission intensity $I(t)$ is proportional to the change in nuclear polarization. Starting from a fully polarized state, SR is due to the increase in the operative HF matrix element $\langle A^+A^-\rangle$. The scale of the coupling is set by $A := g\sum_i g_i$. For a small relative coupling strength $\epsilon = A/(2\Delta)$, where $\Delta := |\Gamma_r/2 + i\omega_S|$, the electron is predominantly in its $|m_S = 0\rangle$ spin state and we can project Eq. (2) to the respective subspace. The reduced master equation for the nuclear density operator reads

$$\dot{\rho} = c_r(A^-\rho A^+ - \tfrac{1}{2}A^+A^-\rho - \tfrac{1}{2}\rho A^+A^-) - ic_i[A^+A^-, \rho] - igm_S[A^z, \rho], \quad (3)$$

where $c_r = g^2/(2\Delta)^2\Gamma_r$ and $c_i = g^2/(2\Delta)^2\omega_S$.

As the electron is optically pumped into $|m_S = 0\rangle$, the last term—representing the electron's Knight field—in Eq. (3) vanishes. Assuming resonance ($\omega_S = 0$) the equation closely resembles the SR master equation which has been discussed extensively in the context of atomic physics [2] and thus SR effects might be expected. However, there is a crucial difference: the inhomogeneous nature ($g_i \neq$ const) of the operators A^μ. They do not preserve the collective spin, affecting the relative phase between nuclei. This could prevent the phased emission necessary for SR [2,11,12]. However, as we shall see, SR is still clearly present in realistic inhomogeneous systems. We take the ratio of the maximum intensity to the initial intensity (the maximum for independent spins) $I_{\mathrm{coop}}/I_{\mathrm{ind}}$ as our figure of merit in the following: if this relative intensity peak height is >1 it indicates cooperative effects.

To see that this effect can be observed at NV centers, we simulate Eq. (2) numerically [13]. The number N of effectively coupled nuclei can range from a few to a few hundred, since the concentration of ^{13}C can be widely tuned [14]. The HF constants g_i between the defect and the nearest ~40 nuclei were derived in [6] in an *ab initio* calculation. Nuclei outside this shell (~7 Å) have a coupling strength gg_i weaker than $2\pi \times 0.5$ MHz and are not considered here. The excited state lifetime of the NV center has been measured as $\tau \approx 13$ ns [15,16]. Thus, we adopt an effective rate $\Gamma_r = 2\pi \times 10$ MHz for the decay from $|m_S = 1\rangle$ to $|m_S = 0\rangle$ enabled by driving the Raman transition. The intensity enhancements predicted by exact simulations for small, randomly chosen, and initially polarized spin environments are shown in Fig. 1(c). In samples of higher ^{13}C concentration N can be larger and stronger effects are expected.

One characteristic feature of SR is the linear N dependence of the associated effects (already visible in Fig. 1). Since the number of nuclei to which the electron couples is much larger in a QD than in a NV center, QDs are particularly attractive candidates for the investigation of SR. In the following we study the dynamics of the QD system in different regimes and we show that strong signatures of SR can be expected in realistic settings.

Let us consider a self-assembled QD in which a single conduction band electron is coupled by isotropic Fermi-contact interaction to a large number of nuclear spins. Optical pumping of the electron is realized by a Raman process, driving a forbidden transition to a trion state [17], and including the HF coupling we again obtain dynamics as sketched in Fig. 1(b). For the optical pumping rate values $\Gamma_r = 2\pi \times (0.1\text{–}1)$ GHz are applicable [18,19]. A comparison with the HF coupling constants reported for different materials [20] shows that for InGaAs and CdSe QDs at resonance Eq. (3) are not valid since the relative coupling strength $\epsilon \geq 1$. We therefore consider the dynamics of the system under conditions of a finite electron inversion [using Eq. (2)]. In this regime, the electron can be seen as a driven and damped two-level system: the nuclei "pump" excitations into the electron, which are damped by the Raman-mediated decay; cooperative behavior manifests in enhanced HF interaction. This enhancement directly translates into increased electron inversion $\langle S^+S^-\rangle$ to which the emitted photon rate is proportional and thus SR from a single QD can be expected. Let us rephrase this, since SR from a *single* emitter is somewhat counter intuitive. Of course, on an optical time scale, antibunched single photons will be emitted at a rate below the optical decay rate. It is, in fact, typically much slower since the emitter is pumped into the optically inactive state $|m_S = 0\rangle$. SR on time scales $\sim 1/\Gamma_r$ consists

thus of lifting this "spin blockade" by HF coupling which becomes increasingly more efficient as nuclear cooperative effects kick in. As in the homogeneous case [2], this enhancement is associated with the transition through nuclear Dicke states $|J, m\rangle$, $|m| \ll J$. Although J is not preserved by inhomogeneous $A^{\pm}$, we can use the Dicke states to illustrate the dynamics. For instance, due to the large homogeneous component in A^{-}, its matrix elements show a strong increase $\propto J$ for states $|J, m\rangle$, $|m| \ll J$.

For large relative coupling strengths $\epsilon \gg 1$ the electron saturates and superradiant emission is capped by the decay rate $\Gamma_r/2$, prohibiting the observation of an intensity burst. In order to avoid this bottleneck regime, we choose a detuning $\omega_S = A/2$ such that $0 < \epsilon = A/\sqrt{\Gamma_r^2 + A^2} \leq 1$. In this parameter range, the early stage of the evolution—in which the correlation buildup necessary for SR takes place [2]—is well described by Eq. (3). The nuclear phasing is counteracted by the dephasing (inhomogeneous) part of the Knight term ($\propto g\sqrt{\mathrm{Var}(g_i)}/2$ [21]), which can cause transitions $J \rightarrow J - 1$. However, the system evolves in a many-body protected manifold (MPM) [22]: The term $\sim[A^{+}A^{-}, \rho]$ energetically separates different total nuclear spin-J manifolds. A rough estimate of the ratio between detuning and dephasing shows a dependence $\propto \epsilon^2$, with proportionality factor >1 (diverging in the homogeneous limit). Thus for values $\epsilon \approx 1$ the correlation buildup should be largely MPM protected. We now confirm these considerations and show by numerical simulation of Eq. (2) that a SR peaking of several orders of magnitude can be observed in the Raman radiation from an optically pumped QD; cf. Fig. 2. An exact numerical simulation of the dynamics is not feasible due to the large number of coupled nuclei and since the dynamics for inhomogeneous coupling cannot be restricted to a low-dimensional subspace. To obtain $I(t) \propto \frac{d}{dt}\sum_i \langle \sigma_i^{+}\sigma_i^{-}\rangle$, we therefore use an approximative scheme. By Eq. (2), these expectation values are related to fourth-order correlation terms involving both the electron and nuclear spins. We use a factorization assumption to reduce the higher-order expressions in terms of the covariance matrix $\gamma_{ij}^{+} = \langle \sigma_i^{+}\sigma_j^{-}\rangle$. Following [23], we apply the bosonic Wick's theorem, incorporating the fermionic character of same-site nuclear spin operators ($[\sigma_i^{+}, \sigma_i^{-}]_{+} = 1$) and replace, e.g., $\langle \sigma_i^{+}\sigma_j^{z}S^{-}\rangle \rightarrow (\gamma_{jj}^{+} - \frac{1}{2}) \times \langle \sigma_i^{+}S^{-}\rangle - \gamma_{ij}^{+}\langle \sigma_j^{+}S^{-}\rangle$. But the electron spin plays a special role and factorizing it completely leads to poor results. Therefore we also solve Eq. (2) for the main higher-order term involving the electron, the "mediated covariance matrix" $\gamma_{ij}^{-} = \langle \sigma_i^{+}S^{z}\sigma_j^{-}\rangle$. All other higher-order expectation values therein are factorized under consideration of special symmetries for operators acting on the same site.

In the regimes accessible to an exact treatment, i.e., the homogeneous case and for few inhomogeneously coupled particles, the factorization results agree well with the exact evolution (see the inset in Fig. 2). This shows that it quantitatively captures the effect of nuclear spin coherences while allowing a numerical treatment of hundreds of spins. Finally, in addition to the constant detuning $\omega_S = A/2$ for the displayed simulations we compensated the Overhauser field dynamically [24]. Furthermore, we assume a Gaussian spatial electron wave function. The results obtained with these methods are displayed in Figs. 2 and 3. For $\epsilon \approx 1$, the strong MPM protection suppresses dephasing, leading to pronounced SR signatures: A strong intensity burst, whose relative height scales $\propto N$ (for large N). For large $\epsilon \approx 1$, the relative height is reduced only by half compared to the ideal Dicke case. For smaller ϵ, it decreases further due to increased dephasing. For $\epsilon \leq 0.3$, where MPM protection is weak and the decay process is significantly slowed down ($c_r \propto \epsilon^2$), even the linear scaling is lost.

From Fig. 3, one extrapolates that for a fully polarized initial state a huge intensity overhead of several orders of magnitude ($\sim 10^3$–10^4) is predicted. If the initial state is not fully polarized, SR effects are reduced. However, even when, e.g., starting from a mixture of symmetric Dicke states $|J, J\rangle$ with polarization $P = 60\%$ [18,25] our simulations predict a strong intensity peak and (for $N \gg 1$) a

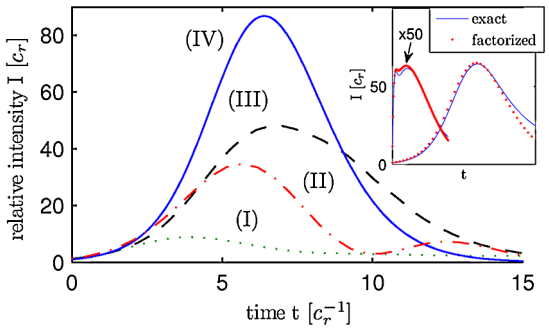

FIG. 2 (color online). Relative intensity under dynamical Overhauser field compensation: $N = 21^2$, $\omega_S = A/2$, and $\epsilon = 0.3$(I), 0.7(II), 0.99(III). (IV) shows the ideal Dicke SR profile [1] as a reference. Inset: comparison of exact evolution and factorization for $N = 9$ inhomogeneously coupled spins (left peak, scaled by factor 50) and $N = 21^2$ homogeneous spins ($\epsilon = 0.7$). Fully independent emitters lead to an exponential curve slowly decaying from 1 to zero and are therefore not depicted.

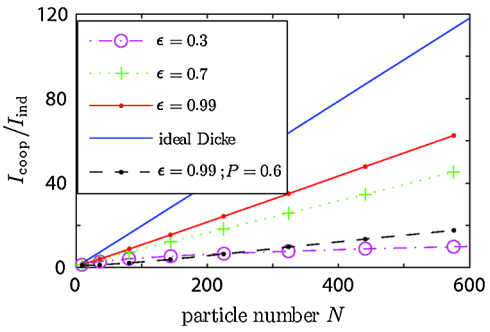

FIG. 3 (color online). $I_{\mathrm{coop}}/I_{\mathrm{ind}}$ for different values of ϵ—the Overhauser field is dynamically compensated and $\omega_S = A/2$ in all cases—compared to the ideal Dicke case. The dashed line corresponds to a partially polarized dot (cf. the text).

linear N dependence: $I_{\mathrm{coop}}/I_{\mathrm{ind}} \approx 0.03N$ ($\epsilon = 0.99$), i.e., only a factor 4 weaker than for full polarization.

Note that for the sake of simplicity, we consider $I = 1/2$ nuclei in our simulations. In terms of particle numbers N, this is a pessimistic assumption as typical QD host materials carry a higher spin. We can incorporate this effect by treating higher spins as $2I$ homogeneously coupled spins $I = 1/2$, thus increasing the effective particle number by the factor $2I$. Most QDs consist of a few different species of nuclei with strongly varying magnetic moments, increasing the inhomogeneity of the system. However, in the worst case the different species evolve independently, diminishing the effect by a small factor corresponding to the number of species. In our simulations, the effect was shown to be much smaller.

We have neglected the dipolar and quadrupolar interaction among the nuclear spins. The former is always negligible on the time scale considered here [5]. The latter is absent for nuclear spin $I = 1/2$ (NV centers, CdSe QDs) or strain-free QDs [18]. In strongly strained QDs it can be important [26], and a term $\sum_i \nu_i (I_i^{z_i})^2$ must be added to Eq. (1), where z_i is defined as the main axis of the local electric-field-gradient tensor.

Having seen that SR can be observed in experimentally accessible nuclear spin ensembles, let us briefly explore two further applications of this setting: nuclear spin polarization and phase transitions. We first note that the master equation Eq. (3) describes optical pumping of the nuclear spins. Its steady states are the eigenstates of A^z, which lie in the kernel of A^-, so-called dark states, and include the fully polarized state. Hence the setting described by Eqs. (2) and (3) can be used to polarize the nuclei [27], i.e., to prepare an initial state required for SR.

Finally, nuclear spin systems may be used to study further cooperative effects such as phase transitions. It is known [3] that in the thermodynamic limit an optically driven atomic system with collective decay—as described by Eq. (3) for homogeneous operators and $m_S = \omega_S = 0$—can undergo a second-order nonequilibrium phase transition in the steady state. In our setting an effective driving can be established by a dc magnetic field B_x perpendicular to the polarization direction. A semiclassical treatment of the equations of motion deduced from Eq. (2) predicts a similar phase transition in the combined system of electron and nuclear spins in certain regimes. Preliminary simulations confirm the validity of the semiclassical results and also indicate the appearance of related phenomena like bistability and hysteresis, which have recently been observed in polarization experiments, e.g., [28]. A detailed analysis of these topics and an analytical description of the SR dynamics presented here will be the subject of a forthcoming publication [29].

In conclusion, we have shown that the nuclear spin environment of individual QDs and NV centers shows superradiant optical emission under suitable optical pumping conditions. While in NV centers a collective intensity enhancement of up to 100% is predicted, the much larger nuclear spin ensembles in QDs could lead to relative peak heights of several orders of magnitude. This would be clear evidence of coherent HF dynamics of nuclear spin ensembles in QDs. The rich physics of SR systems, including bistability and phase transitions, could thus be studied in a long-lived mesoscopic solid-state system.

We acknowledge support by GIF, the DFG within SFB 631 and the Cluster of Excellence NIM, the NSF, DARPA, and the Packard Foundation.

[1] R. H. Dicke, Phys. Rev. **93**, 99 (1954).
[2] M. Gross and S. Haroche, Phys. Rep. **93**, 301 (1982).
[3] H. J. Carmichael, J. Phys. B **13**, 3551 (1980).
[4] S. Morrison and A. S. Parkins, Phys. Rev. A **77**, 043810 (2008).
[5] J. Schliemann *et al.*, J. Phys. Condens. Matter **15**, R1809 (2003).
[6] A. Gali *et al.*, Phys. Rev. B **77**, 155206 (2008).
[7] F. Jelezko and J. Wrachtrup, Phys. Status Solidi A **203**, 3207 (2006).
[8] M. V. G. Dutt *et al.*, Science **316**, 1312 (2007); P. Neumann *et al.*, Science **320**, 1326 (2008).
[9] A field of ~100 mT is sufficient to compensate the zero-field splitting between $|m_S = 1\rangle$ and $|m_S = 0\rangle$.
[10] P. Tamarat *et al.*, New J. Phys. **10**, 045004 (2008).
[11] C. Leonardi and A. Vaglica, Nuovo Cimento Soc. Ital. Fis. B **67**, 256 (1982).
[12] G. S. Agarwal, Phys. Rev. A **4**, 1791 (1971).
[13] Equation (2) allows for the full incorporation of anisotropies.
[14] A. T. Collins *et al.*, J. Phys. C **21**, 1363 (1988).
[15] A. Lenef *et al.*, Phys. Rev. B **53**, 13427 (1996).
[16] A. T. Collins *et al.*, J. Phys. C **16**, 2177 (1983).
[17] *Semiconductor Quantum Bits* edited by F. Henneberger and O. Benson (Pan Stanford Publishing, Singapore, 2009).
[18] A. Bracker *et al.*, Phys. Rev. Lett. **94**, 047402 (2005).
[19] G. Finkelstein *et al.*, Phys. Rev. B **58**, 12637 (1998); P. A. Dalgarno *et al.*, Appl. Phys. Lett. **89**, 043107 (2006).
[20] The HF coupling constants and typical numbers of nuclei (A/μeV, N) for important QD materials are [5,17] GaAs:(100, 10^4–10^6), CdSe:(10, 10^3), SiP:(0.1, 10^2).
[21] V. V. Temnov and U. Woggon, Phys. Rev. Lett. **95**, 243602 (2005).
[22] A. M. Rey *et al.*, Phys. Rev. A **77**, 052305 (2008).
[23] A. V. Andreev *et al.*, *Cooperative Effects in Optics* (IOP Publishing, Bristol, 1993).
[24] By applying a time dependent magnetic or spin-dependent AC Stark field such that $\omega_S(t) = g\langle A^z\rangle_t$, we ensure that the measured change in radiation intensity is due to a cooperative emission effect only.
[25] P. Maletinsky, Ph.D. thesis, ETH Zürich, 2008, http://e-collection.ethbib.ethz.ch/view/eth:30788.
[26] P. Maletinsky *et al.*, Nature Phys. **5**, 407 (2009).
[27] H. Christ *et al.*, Phys. Rev. B **75**, 155324 (2007).
[28] A. I. Tartakovskii *et al.*, Phys. Rev. Lett. **98**, 026806 (2007); P.-F. Braun *et al.*, Phys. Rev. B **74**, 245306 (2006); C. Latta *et al.*, Nature Phys. **5**, 758 (2009).
[29] E. M. Kessler *et al.* (unpublished).